01,11

Electrical resistance of $Ni_{42+x}Mn_{47-x}Sn_{11}$ alloys

© N.V. Volkova, V.V. Chistyakov, E.I. Patrakov, P.S. Korenistov, A.N. Perevalova, S.M. Emelyanova

M.N. Mikheev Institute of Metal Physics, Ural Branch, Russian Academy of Sciences, Yekaterinburg, Russia

E-mail: nvolkova@imp.uran.ru

Received November 18, 2021
Revised November 18, 2021
Accepted November 23, 2021

The electrical resistance and structure of $Ni_{42+x}Mn_{47-x}Sn_{11}$ alloys have been studied; where $x = 0, 1, 2, 3, 4$, At room temperature, $Ni_{42+x}Mn_{47-x}Sn_{11}$ alloys are ordered in the cubic $L2_1$ Ni_2MnSn structure characteristic of Heusler alloys. The phase transition between the cubic austenite phase and martensite with lower symmetry, characteristic of ferromagnetic non-stoichiometric Heusler alloys, is observed at temperatures below room temperature. It was found that the partial replacement of Mn atoms by Ni atoms leads to an increase in the phase transition temperatures and to their shift to room temperature.

Keywords: Heusler alloys, electrical resistance, phase transition.

DOI: 10.21883/PSS.2022.03.53184.244

1. Introduction

Research of „smart " materials are becoming relevant at the present time. „Smart" are multifunctional materials that have a set of controlled physical characteristics. In such materials, the controlled significant change in one or more properties is observed in response to changes in external conditions. The change in properties is reversible and can be repeatedly reproduced under cyclic exposure to the external environment. To date, the most well-known multifunctional materials include Heusler alloys, which can have a shape memory effect and the magneto-caloric effect (MCE). When working with such alloys, it is possible to obtain the required functional properties by varying the chemical composition of the samples.

Ferromagnetic (FM) Heusler alloys are intermetallic compounds ordered in a cubic $L2_1$ structure. It is known [1,2] that FM Heusler alloys based on Ni-Mn undergo the first-order phase transition between the low-temperature martensitic phase and the high-temperature austenite phase, which is accompanied by the sharp change in magnetization and electrical resistance. In $Ni_{47-x}Mn_{42+x}In_{11}$ ($x = 0, 1, 2$) alloys, this transition and large MCE values are observed in the room temperature region, [3]. This makes these alloys promising for use as a refrigerant. In the work [4], $Ni_{50-x}Mn_{39+x}Sn_{11}$ alloys, where $x = 5, 6, 7$, were studied. From the temperature dependences of the magnetization in weak fields, the characteristic temperatures of phase transitions are determined: M_s and M_f — the beginning and end of the martensitic transformation, A_s and A_f — the beginning and end of the austenitic transformation, as well as the Curie temperature of the martensitic and austenitic phases. It has been found that an increase in the Mn concentration shifts the phase transition to the region of low temperatures. In the studied concentration range, phase transitions are observed at temperatures below room temperature.

The aim of this work was to search for Heusler alloys based on Ni-Mn in which a large MCE is observed at room temperature. For this, five $Ni_{42+x}Mn_{47-x}Sn_{11}$ samples were made, where $x = 0, 1, 2, 3, 4$. The amount of tin did not change, and nickel atoms partially replaced manganese atoms.

The article is organized as follows. Section 2 describes the experimental procedures used in this work. Section 3 investigates the structure and electrical resistance of $Ni_{42+x}Mn_{47-x}Sn_{11}$ alloys, where $x = 0, 1, 2, 3, 4$. The last section is devoted to conclusions.

2. Experimental part

$Ni_{42+x}Mn_{47-x}Sn_{11}$ alloys, where $x = 0, 1, 2, 3, 4$, were smelted in an arc furnace in the atmosphere argon. The obtained ingots were annealed in the quartz flask in the helium atmosphere at temperature of 1100 K for 96 h. The annealing was not carried out continuously, with cooling to room temperature for about 11 hours and subsequent heating to 1100 K for a time of about 13 h. At the end of annealing, water quenching was carried out. The ingots were cut by the electric spark method. Then powders were prepared for X-ray diffraction studies. Electrical resistance measurements were carried out by the standard four-contact method at the constant switched current of 25 mA in the heating mode and subsequent cooling in the temperature ranges below room temperature from 77 to 340 K and above room temperature from 290 to 1100 K.

Analysis of the chemical composition of the alloy was carried out using an electron scanning microscope with an FEI Inspect F field emission cathode and the GENESIS

Spectrum attachment (Inspect F, FEI Company) with an EDAX spectrometer.

The structure of the alloy was studied by the Department of X-ray diffraction analysis of the Center for Collective Use of the M.N. Mikheev Institute of Metal Physics, Ural Branch of Russian Academy of Sciences using the „Empyrean" high-resolution X-ray diffractometer (manufactured by PANalytical) in copper filtered radiation by scanning with the step of 0.02° at room temperature in the angle range from 20 to 100 deg. Primary processing and calculation of parameters were carried out using the HighScore Plus 4.1 software package.

3. Results and discussion

The analysis of the chemical composition of the ingots, carried out using an electron scanning microscope before ordering annealing, showed that the chemical composition corresponds to the nominal one. The surface of the ingots is quite homogeneous. Ordering annealing at 1100 K for 24 hours led to the appearance of small areas with Mn content above 90%, then ordering annealing at 1100 K for 96 h led to a decrease in these areas or to disappearance.

Figure 1 shows X-ray diffraction patterns of $Ni_{42+x}Mn_{47-x}Sn_{11}$ alloy samples, where $x = 0$, 1, 2, 3, 4. The observed diffraction peaks are related to the FCC-phases of Ni_2MnSn (on the order of 50%) and MnNi. Partial replacement of Ni atoms by Mn atoms leads to a decrease in the fraction of the Ni_2MnSn phase in the bulk of the sample and, accordingly, to an increase in the fraction of MnNi.

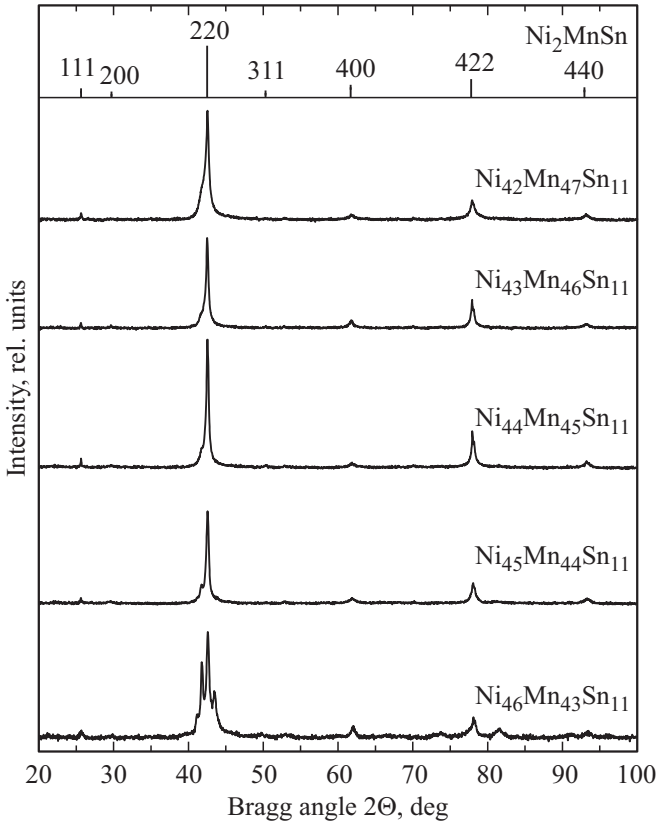

Figure 1. X-ray diffraction patterns of $Ni_{42+x}Mn_{47-x}Sn_{11}$ alloy samples, where $x = 0$, 1, 2, 3, 4.

The temperature dependences of electrical resistivity of $Ni_{42+x}Mn_{47-x}Sn_{11}$ alloy samples at temperatures from 77 to 1100 K are shown in Fig. 2. For all samples at temperatures below room temperature, features are observed that probably indicate a structural phase transition of the first order, accompanied by hysteresis inherent in similar alloys of nonstoichiometric composition Ni-Mn-X (X = Ga, In, Sn, Sb) [3–5].

In the entire temperature range above the detected features, a positive TCR (temperature coefficient of resistance) is observed. However, the increase in resistivity with increasing temperature differs from the linear one characteristic of metals. As can be seen in Figs. 2 and 3, the so-called saturation effect is observed. The latter consists in the fact that a negative curvature of the temperature dependence of the electrical resistance is observed, i.e., TCR decreases with increasing temperature. This phenomenon has been observed in various alloys, in particular Ni_3Mn, and may be due to the approach of the mean free path to the value of the interatomic distance [6].

For the $Ni_{43}Mn_{46}Sn_{11}$ sample, during cooling at a temperature of about 460 K, a peculiarity in the form of an inflection, is observed in the temperature dependence of the electrical resistance. When heated, this feature is not observed. The rate of heating and cooling does not affect the observation of this phenomenon. The temperature dependence of the electrical resistance and TCR of the $Ni_{43}Mn_{46}Sn_{11}$ alloy at high temperatures is shown in Fig. 3. As a rule, similar features (denoted by a vertical line) on the temperature dependences of the electrical resistance associated with structural and magnetic transformations are observed both during heating and cooling. The electrical resistivity value coincides with repeated heating up to 1100 K and subsequent cooling. This indicates that ordering annealing for 4 days led to the achievement of an equilibrium structural state.

Temperature dependence of the electrical resistance of a $Ni_{43}Mn_{46}Sn_{11}$ alloy sample at low temperatures from 77 to 300 K is shown in Fig. 4. The work [7] presents the results of measurements of the temperature dependence of the magnetization and heat capacity of the $Ni_{43}Mn_{46}Sn_{11}$ alloy in various magnetic fields. The sample was annealed at 1073 K for 24 h followed by quenching in water. The austenite-martensite phase transition, accompanied by a jump in heat capacity, was observed at temperatures of 200 K and below, and the transition temperature decreased with increasing magnetic field.

As can be seen in Fig. 2, for the $Ni_{46}Mn_{43}Sn_{11}$ sample, upon cooling from high temperatures, the curve of the temperature dependence of the electrical resistance intersects the curve upon heating approximately at 350 K. The slope

of the curve is flatter than for other samples. For this sample, the peaks related to the MnNi phase become more distinct on the X-ray diffraction pattern, and, accordingly, the amount of this phase is maximum. The probable temperatures of the beginning and end of the austenitic and martensitic transformation, determined by the tangent intersection method, are shown in Fig. 5. It can be seen that an increase in the Ni concentration leads to an increase in

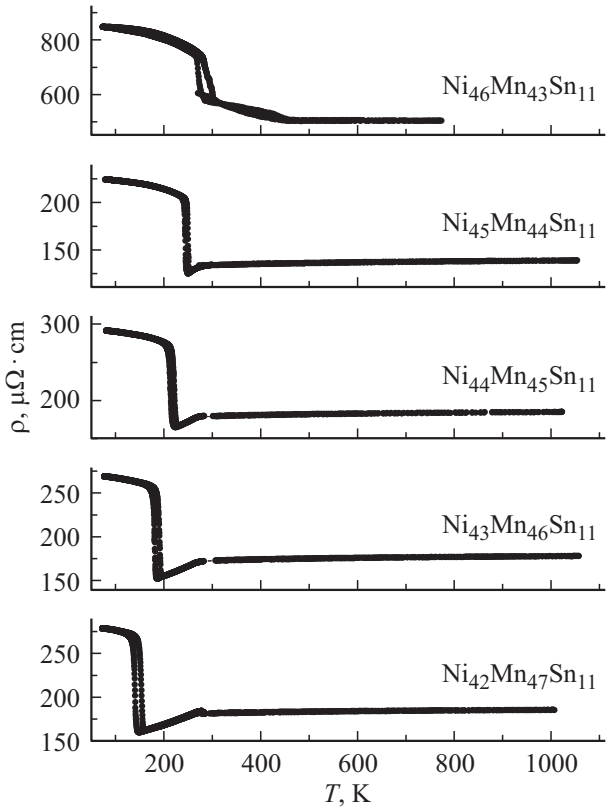

Figure 2. Temperature dependences of electrical resistance of $Ni_{42+x}Mn_{47-x}Sn_{11}$ alloy samples, where $x = 0$, 1, 2, 3, 4 from 77 to 1100 K.

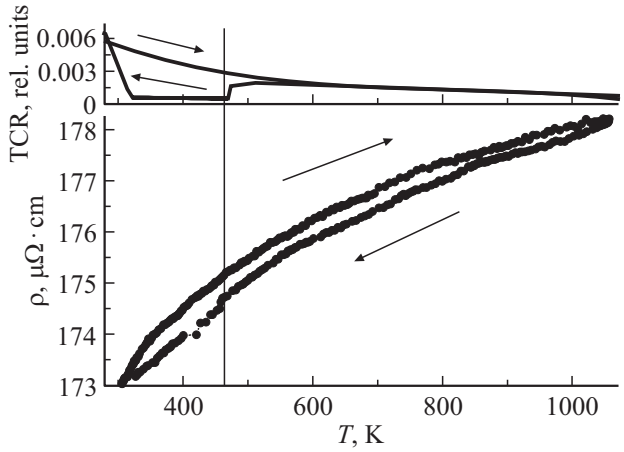

Figure 3. Temperature dependence of the electrical resistance and TCR of a $Ni_{43}Mn_{46}Sn_{11}$ alloy sample at high temperatures from 300 to 1100 K.

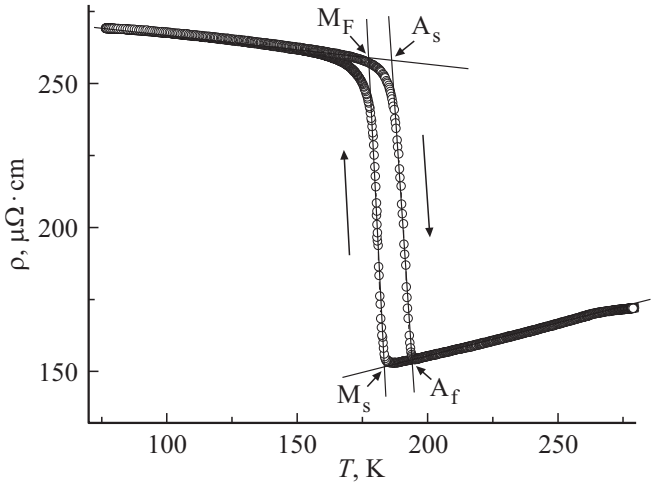

Figure 4. Temperature dependence of the electrical resistance of a $Ni_{43}Mn_{46}Sn_{11}$ alloy sample at low temperatures from 77 to 300 K.

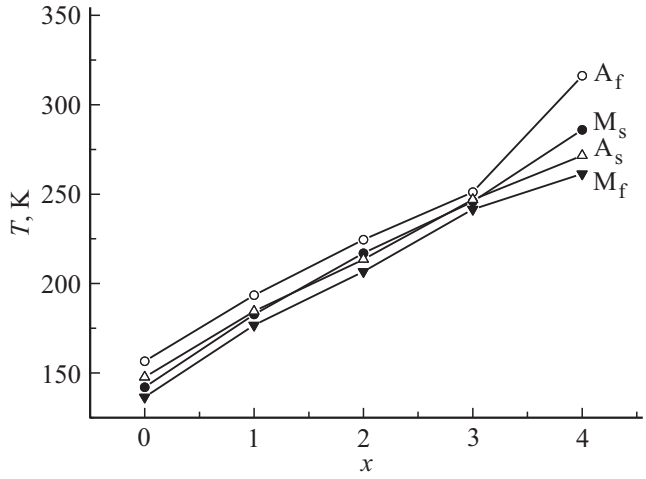

Figure 5. Concentration dependence of characteristic temperatures of phase transformations of $Ni_{42+x}Mn_{47-x}Sn_{11}$ alloy samples, where $x = 0$, 1, 2, 3, 4. M_s and M_f — temperatures of the beginning and end of martensitic transformation, A_s and A_f — temperatures of the beginning and end of austenitic transformation.

the phase transition temperatures. For an alloy with $x = 4$, the phase transition is observed at room temperature.

If the study of magnetic properties reveals high values of the MCE in these alloys, as was found in [3–5,8], this alloy may be promising for use as a cooling agent.

4. Conclusion

Conducted research have shown that $Ni_{42+x}Mn_{47-x}Sn_{11}$ alloys, where $x = 0$, 1, 2, 3, 4, are ordered in cubic $L2_1$ structure, consist of a mixture of two phases: Ni_2MnSn (about 50%) and MnNi. The increase in x leads to a decrease in the amount of the Ni_2MnSn phase and the increase in the amount of the MnNi phase. This is

accompanied by the increase in the probable temperatures of the first-order phase transition austenite–martensite and their shift to room temperature. The selection of such a composition was the goal of this work. Further studies of the magnetic properties of these alloys are advisable from the point of view of searching for materials with a high MCE value in the room temperature region.

Acknowledgments

The authors are grateful to Mr. V.V. Marchenkov for the idea and provided samples, to Mr. V.S. Gaviko for X-ray diffraction studies, and to Mr. A.F. Prekul for help with sample annealing and useful discussion.

Funding

The work has been performed under the state assignment of the Ministry of Science and Higher Education of the Russian Federation (topic „Spin“ No. AAAA-A18-118020290104-2).

Conflict of interest

The authors declare that they have no conflict of interest.

References

[1] Y. Sutou, Y. Imano, N. Koeda, T. Omori, R. Kainuma, K. Ishida, K. Oikawa. Appl. Phys. Lett. **85**, 4358 (2004).
[2] N.H. Dan, N.H. Duc, N.H. Yen, P.T. Thanh, L.V. Bau, N.M. An, D.T.K. Anh, N.A. Bang, N.T. Mai, P.K. Anh, T.D. Thanh, T.L. Phan, S.C. Yu. J. Magn. Magn. Mater. **374**, 372 (2015).
[3] S.M. Emelyanova, V.V. Marchenkov, K.A. Belozerova, E.I. Patrakov, R.L. Wang, H.B. Xiao, C.P. Yang, H.W. Weber, F. Sauerzopf, Yu.V. Kaletina. Solid State Phenomena **233–234**, 233 (2015).
[4] Z.D. Han, D.H. Wang, C.L. Zhang, H.C. Xuan, B.X. Gu, Y.W. Du. Appl. Phys. Lett. **90**, 042507 (2007).
[5] S.M. Emelyanova, N.G. Bebenin, V.P. Dyakina, V.V. Chistyakov, T.V. Dyachkova, A.P. Tyutyunnik, R.L. Wang, C.P. Yang, F. Sauerzopf, V.V. Marchenkov. PMM **119**, *2*, 130 (2018).
[6] A.S. Shcherbakov, N.I. Kourov, Yu.N. Tsiovkin. Physics of the Solid State **27**, *6*, 1685 (1985).
[7] V.V. Sokolovsky, D.V. Nachinova, V.D. Buchelnikov, Z.T. Dilmieva, Yu.S. Koshkidko, S.M. Emelyanova, E.B. Marchenkova, V.V. Marchenkov. Chelyabinskiy fiz.-mat. zhurn. **5**, 493 (2020) (in Russian).
[8] Kourov N.I., Marchenkov V.V., Korolev A.V., Stashkova L.A., S.M. Emelyanova, H.W. Weber. Physics of the Solid State **57**, *4*, 684 (2015).